Smart Structures and Systems, *Vol. 20, No. 1 (2017) 23-33*
DOI: https://doi.org/10.12989/sss.2017.20.1.023

Sensitivity analysis of variable curvature friction pendulum isolator under near-fault ground motions

Parisa Shahbazi and Touraj Taghikhany*

Department of Civil and Environmental Engineering, Amirkabir University of Technology (Tehran Polytechnic), Tehran, Iran

(Received May 21, 2016, Revised June 12, 2017, Accepted June 14, 2017)

Abstract. Variable Curvature Friction Pendulum (VCFP) bearing is one of the alternatives to control excessive induced responses of isolated structures subjected to near-fault ground motions. The curvature of sliding surface in this isolator is varying with displacement and its function is non-spherical. Selecting the most appropriate function for the sliding surface depends on the design objectives and ground motion characteristics. To date, few polynomial functions have been experimentally tested for VCFP however it needs comprehensive parametric study to find out which one provides the most effective behavior. Herein, seismic performance of the isolated structure mounted on VCFP is investigated with two different polynomial functions of the sliding surface (Order 4 and 6). By variation of the constants in these functions through changing design parameters, 120 cases of isolators are evaluated and the most proper function is explored to minimize floor acceleration and/or isolator displacement under different hazard levels. Beside representing the desire sliding surface with adaptive behavior, it was shown that the polynomial function with order 6 has least possible floor acceleration under seven near-field ground motions in different levels.

Keywords: seismic isolation; variable curvature friction pendulum; sensitivity analysis; near-fault ground motion

1. Introduction

Sliding isolator besides dissipating input energy cuts the maximum acceleration off to the friction coefficient. As a consequent, it makes superstructure relatively insensitive to variations of the frequency content and amplitude of the input excitation (Mostaghel and Tanbakuchi 1983). Nevertheless, lack of significant restoring force results permanent offset displacement of the superstructure. To avoid this unsatisfactory feature, Zayas *et al.* (1990) introduced spherical sliding surface with constant radius of curvature named as Friction Pendulum System (FPS). FPS uses gravity action to supply restoring force, however its relatively constant time period of oscillation limits its efficiency under broad range of ground excitation (Sinha and Pranesh 1998).

In order to improve the seismic performance of FPS and provide an adaptive device many innovative concepts have been introduced. One of these ideas is using multi-spherical sliding bearings, which consists of more than one concave surface; thereby it shows different hysteresis behavior as the slider slides on more than one concave. Number of authors such as Fenz and Constantinou have investigated the mechanical behavior of these isolators (Fenz 2008, Fenz and Constantinou 2008a, Moeindarbari and Taghikhany 2014, Fallahian *et al.* 2015). However multi-spherical sliding bearings have the negative effect of impact when the slider contacts the displacement restrainer (Fenz 2008).

To overcome the above mentioned challenges, Tsai *et al.* (2004) introduced spherical sliding isolator which its coefficient of friction varies continuously with isolator displacement. Further studies confirm the adaptive behavior of this system (Panchal and Jangid 2008a, b, Kong *et al.* 2014, Calvi and Ruggiero 2016), however dependency of the friction coefficient to intractable parameters is a serious impediment to application of these isolators in practice.

Another effort to introduce an adaptive isolation system has been made by Fakhouri and Igarashi through proposing multiple-slider surfaces bearing (Fakhouri and Igarashi 2013). It is a simple sliding device consisting of one horizontal and two inclined plane sliding surfaces at both ends set in series. They investigated the application of such bearings for seismic retrofitting of frame structures with soft first stories. The numerical results show reduction of ductility demand and excessive drift for the first story columns.

A recent solution found to be efficient and practicable is Variable Curvature Friction Pendulum (VCFP). It consists of a sliding surface and an articulated slider, resembling FPS isolator, except that the sliding surface is non-spherical and has a variable curvature. As a result, isolation system has not constant period of vibration and it varies along with the isolator displacement. Pranesh and Sinha (2000), and Tsai *et al.* (2003) evaluated the performance of VCFP isolators using an elliptical sliding surface that its major axis extends as the slider takes away from the center point of sliding surface. So the period of oscillation was increasing with isolator displacement and its behavior was varying between FPS and pure friction (PF) isolator. They showed that the possibility of low-frequency resonant can be attenuated but it leads to excessively large lateral and

*Corresponding author, Ph.D.
E-mail: ttaghikhany@aut.ac.ir

Copyright © 2017 Techno-Press, Ltd.
http://www.techno-press.com/journals/sss&subpage=7
ISSN: 1738-1584 (Print), 1738-1991 (Online)

residual displacements. It displayed stable performance during low-intensity excitations, and fail-safe during high-intensity excitations. In different studies, Lu *et al.* (2006) and Gillich *et al.* (2012) introduced VCFP isolators with polynomial function as sliding surface. Lu et al. conducted experimental tests to verify the efficiency of fourth and sixth order polynomial functions. They showed effectiveness of these sliding surfaces to suppress the isolator displacement and inter-story acceleration under near-fault ground motion.

In more recent researches by Lu *et al.* (2013) the application of VCFP bearing in isolated raised floor was investigated experimentally with sixth order polynomial function. Further studies, exhibited adoptive hysteretic behavior of Variable Frequency Rocking Bearing (VFRB) with polynomial function as rocking surface (Lu and Hsu 2013). They had no sensitivity analysis on the parameters of selected function and attempt to optimally determination of design parameters.

The appropriate function for the sliding surface depends on the design objectives and ground motion characteristics. The philosophy of the performance based design of seismic isolators is controlling the maximum floors acceleration during low and intermediate ground motion levels and limiting lateral displacement of the isolator in large scale ground motions. To achieve these targets the mathematical function should provide a restoring force with variation between softening and hardening phase. In other words, the derivation of mathematical function should have incremental trend when the slider moves away from its neutral position (Shahbazi *et al.* 2013, Shahbazi and Taghikhany 2014).

Variation of the first derivative of the fourth and sixth order polynomial functions in Fig. 1 confirms that the normalized restoring force of fourth and sixth order polynomial functions beside initial stiffness k_0 depends on the other parameters as D and k_D. To date, the reported results about different functions are related only to specific values of constant parameters. To understand the role of theses parameters as; D , k_D and k_0 a sensitivity analysis in different levels of ground motion is necessary.

Herein, seismic performance of the isolated structure mounted on VCFP is investigated with two different polynomial functions of the sliding surface. In order to determine the effective parameters of chosen functions a sensitivity analysis is developed by using a set of near-field ground motions. The most proper combination of design parameters function is explored to minimize floor acceleration and/or isolator displacement.

2. Variable Curvature Friction Pendulum (VCFP) Isolator

2.1 Mathematical model

Similar to a conventional friction pendulum system, a VCFP isolator primarily consists of a slider and a concave sliding surface to uncouple the super-structure motion from the ground excitation. However, VCFP has variable curvature and its restoring stiffness and isolation frequency are changing with the isolator displacement.

Fig. 2 shows the top view of the sliding curvature and free-body diagram of a VCFP. The cross-section of the sliding surface in this figure is defined by a geometric function y(x) in the x-y coordinates. In accordance with Lu *et al*. (2011) the isolator shear force of the sliding surface with variable curvature can be written as

$$F_s(x) = F_r(x) + F_f(x) \tag{1}$$

$$F_r(x) = wy'(x) \tag{2}$$

$$F_f(x) \approx \mu W sign(\dot{x}) \tag{3}$$

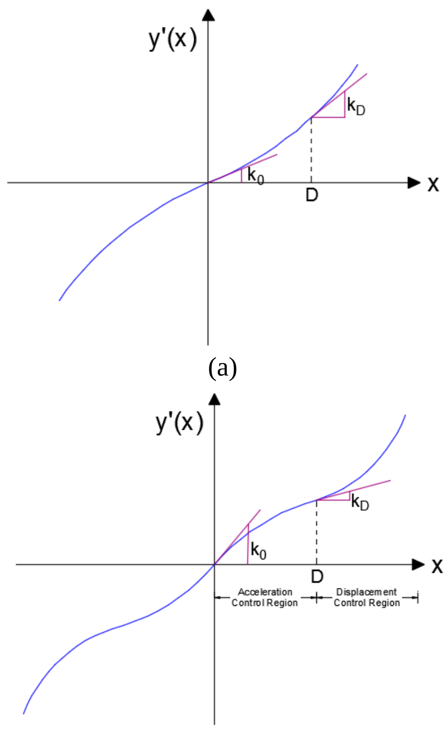

(a)

(b)

Fig. 1 Variation of *y′(x)* (normalized restoring force) for (a) fourth and (b) sixth order polynomial functions

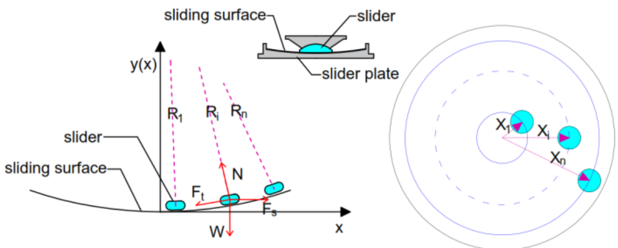

Fig. 2 Free body diagram and top view of the sliding curvature of VCFP isolator

Where $F_r(x)$ and $F_f(x)$ denote the restoring force and the friction force respectively. *W* is the total weight of the super-structure. *y'(x)* is the first derivate of the geometric function *y(x)*. The isolator stiffness $k_r(x)$, which is the rate of change of the restoring force $u_r(x)$, and the tangential isolation frequency $\omega(x)$ further computed by Eqs. (4) and (5) (Lu *et al.* 2011).

$$k_r(x) = Wy''(x) \tag{4}$$

$$\omega(x) = \sqrt{gy''(x)} \tag{5}$$

As Eqs. (2), (4) and (5) show, $F_r(x)$, $k_r(x)$ and $\omega(x)$ are varying with slider displacement *x* and depends on geometric function *y(x)* which is the main difference of a VCFP with a conventional sliding isolation system (Lu *et al.* 2011).The coefficient of friction in Eq. (3) is velocity dependent and described as (Constantinou *et al*. 1990)

$$\mu = f_{max} - (f_{max} - f_{min})\exp(-a|\dot{x}|) \tag{6}$$

Where $|\dot{x}|$ is the sliding velocity, f_{max} and f_{min} are the sliding coefficients of friction at large velocity and nearly zero sliding velocity, respectively and α is a rate parameter that controls the transition from f_{min} to f_{max}. α is considered to be 100 s/m for single concave bearings (Constantinou *et al.* 1990) and 50 m/s for each sliding surface of double concave isolator.

The maximum floor acceleration and peak displacement of isolator are computed by state space formulation of the Equations of motion in MATLAB using ODE function and application of Runge-Kutta method.

2.2 Verification of the numerical model

In order to verify modeling of structure and results, the introduced single-story structure mounted on VCFP by Pranesh and Sinha is modeled and its time history responses are compared in Fig. 3. Time period of fixed-base structure is 0.5 second and its damping ratio is taken as 2 percent of critical value. The mass of first and base floors are taken equal, so that the mass ratio is 0.5. The initial period of 2 seconds and friction coefficient of 0.02 is chosen for VCFP and the mathematical function of sliding surface based on the expression of an ellipse is (Pranesh and Sinha 2000):

$$y = 0.01\left[1 - \frac{\sqrt{0.01 + 0.2x}}{0.1 + x}\right] \tag{7}$$

The structure is subjected to NS component of El Centro 1940 (NS) ground motion scaled by factor 2.

In addition, to verify the numerical model of VCFP with sixth-order polynomial geometric function, time history displacement of isolator and its hysteretic curve are compared in Fig. 4 with experimental and numerical results reported by Lu *et al*. under Imperial Valley ground motion (Lu *et al.* 2011). The super structure is a full-scale one-story steel frame with height of three meters and weight equal 12 metric tons. It had a fundamental frequency (fixed base) of 2.33 Hz and a damping ratio of 2%. The initial stiffness k_0 is chosen in relation to initial isolation period equal to one second. The isolator stiffness k_D at inflection point D is about 1.5 times of the initial stiffness. As it shown in Fig. 1, the inflection point is the switching mark between the acceleration and displacement control region (softening and hardening) in sixth-order polynomial geometric function (O6) isolator and it assists to achieve definite performance objective in specific seismic levels.

Figs. 3 and 4 show that the numerical model used in this study has sufficient accuracy to simulate dynamic response of VCFP with different sliding surface functions.

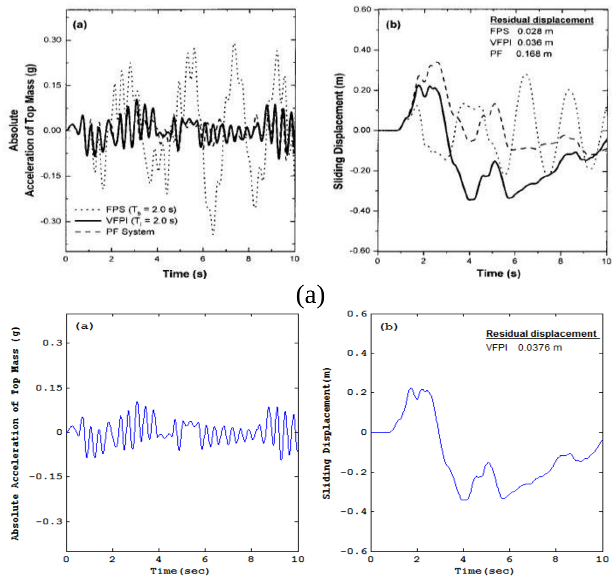

Fig. 3 Comparison of time history responses of VCFP isolator governed by (a) Pranesh and Sinha (Pranesh and Sinha 2000) (black colors) and (b) MATLAB analysis (blue colors)

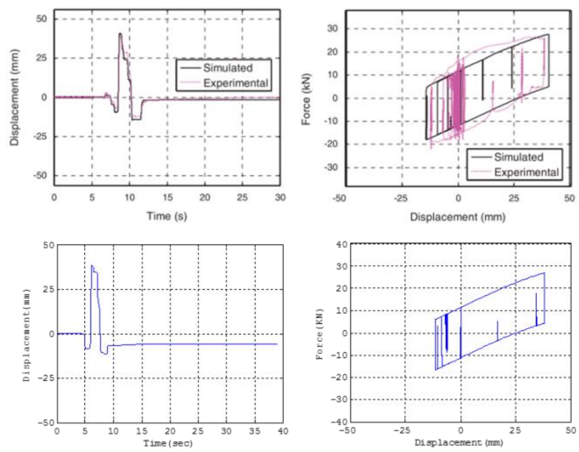

Fig. 4 Comparison of time history responses of VCFP isolator governed by (Lu *et al.* 2011) (black and pink colours) and MATLAB analysis (blue colours)

Table 1 Geometric functions used for VCFP isolators, and their first and second derivate

Function	$y(x)$	$y'(x)$	$y''(x)$
O4	$p_1x^4 + p_2x^2$	$4p_1x^3 + 2p_2x$	$12p_1x^2 + 2p_2$
O6	$q_1x^6 + q_2x^4 + q_3x^2$	$6q_1x^5 + 4q_2x^3 + 2q_3x$	$30q_1x^4 + 12q_2x^2 + 2q_3$

3. Design parameters in geometric function

As it described earlier, to achieve design objectives of seismic isolated buildings the mathematical function for sliding surface should provide a restoring force with variation between softening and hardening phase. Herein, seismic performance of VCFPs with two different sliding curvatures; fourth and sixth order polynomial functions which are denoted respectively by "O4" and "O6", are investigated. Their geometric functions, first and second derivatives are listed in Table 1.

For design purposes, it is necessary to have engineering interpretation for the mathematical coefficients in this Table (p_1,p_2,q_1,q_2,q_3).To this end, these coefficients are defined by introduced engineering parameters as; initial stiffness (k_0), specific displacement D with its related stiffness as k_D. Eqs. (8) and (9) for O4 isolator and Eqs. (10)-(12) for O6 isolator display the relation between their coefficients and engineering parameters.

$$p_1 = \frac{k_D - k_0}{12D^2} \tag{8}$$

$$p_2 = \frac{1}{2}k_0 \tag{9}$$

$$q_1 = \frac{k_0 - k_D}{30D^4} \tag{10}$$

$$q_2 = \frac{k_D - k_0}{12D^2} \tag{11}$$

$$q_3 = \frac{1}{2}k_0 \tag{12}$$

Where k_0, the normalized initial stiffness at $x=0$ is computed by Eq. (13).

$$k_0 = \left(\frac{2\pi}{T_0}\right)^2 / g \tag{13}$$

According to Table 1 and Eqs. (8)-(12) in order to have a polynomial function of order 4 or 6, k_0 should not be equal to k_D. Otherwise the sliding surface would have a circular surface just like a conventional FPS isolator. An example of such selection is presented in section 5.3.

Fig. 5 shows schematic hysteresis loop of VCFP isolators with two different sliding surface functions under a sinusoidal loading. The initial period, minimum friction coefficient and specific displacement of both systems are 2 sec, 0.065 and 0.2 meters, respectively. As shown in hysteretic loops, the inflection point of the O6 sliding function is clearly separate two different regions.

In order to study the effect of variation of D on seismic behavior of VCFP, a sensitivity analysis is performed on both O4 and O6 isolators. Here, the values for D are selected as a ratio of design displacement of isolators for specific site. The design displacement in accordance with recommendation of FEMA 450 is calculated by (FEMA 2003)

$$D_D = \left(\frac{g}{4\pi^2}\right)\frac{S_{D1}T_D}{B_D} \tag{14}$$

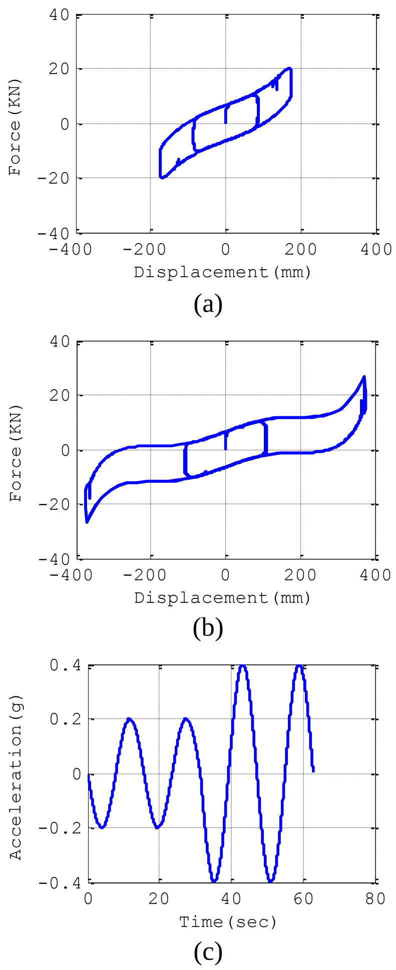

Fig. 5 Schematic hysteresis loop of VCFP isolators under sinusoidal loading. (a) fourth order function (O4), (b) sixth order function (O6) and (c) load pattern

Where T_D is effective period, B_D is damping reduction factor and S_{D1} is design spectral acceleration at one second. In this study, the design displacement are calculated for a site with soil type C, spectral response acceleration parameter $S_I = 0.40$ and isolator parameters as $B_D = 1$ and $T_D = T_0$. For five different initial periods equal to 1,2,3,4 and 5 seconds the design displacements respectively are 0.09, 0.19, 0.28, 0.37 and 0.46 meters.

Here by selecting specific displacement (D) equal to 0.1, 0.2 and 0.3 meter, we have isolators with D which its value ranges between 0.2 and 3 times of each design displacements (D_D). The isolators with related functions and D values are denoted by "O4-1, O4-2 and O4-3" and "O6-1, O6-2 and O6-3" in this study.

As shown in Fig. 1, the normalized isolator stiffness at D, k_D, in O4 isolator is assumed equal to 4 and this parameter for O6 isolator is assumed equal to 0 (1/m). It is noteworthy, though k_D, is assumed as specific value, by variation of D, the position of normalized isolator stiffness is changing and consequently the stiffness at previous point is not similar. Table 2 summarized the assumptions for D and k_D in different VCFP isolators.

To have better understanding on D variation effects, besides initial stiffness, the response of each VCFP isolator are evaluated for the range of minimum friction coefficient from 0.02 to 0.065. In all models the maximum friction coefficient are assumed as two times of the selected minimum coefficient. As it listed in Table 3, seismic performances of 120 VCFPs are investigated for two different polynomial functions. These results are compared with dynamic response of FPS isolators with similar period of vibrations and friction coefficients.

The considered super-structure is one story building with total weight of 133.33 kN, and fundamental period as 0.20 second with damping ratio equal to 0.025. This superstructure is assumed to be mounted on four similar friction pendulum bearing. This model has been previously tested by Fenz and Constantinou (Fenz and Constantinou 2008b) to evaluate the seismic performance of Triple concaves Friction Pendulum Bearings.

4. Near-fault ground motions

The imperfection of conventional sliding isolation systems is revealed when they are subjected to near-field ground motions having strong pulses, with eventuating excessive displacements because of resonance.

Table 2 Design assumptions for VCFP isolators

Isolator		Assumptions	
Function	Name	*D (m)*	k_D *(1/m)*
Order 4 polynomial function	O4-1	0.1	4
	O4-2	0.2	4
	O4-3	0.3	4
Order 6 polynomial function	O6-1	0.1	0
	O6-2	0.2	0
	O6-3	0.3	0

Table 3 Chosen properties for VCFP cases

Case no.	Minimum Friction Coefficient	Initial Period (sec.)
1		1
2		2
3	0.02	3
4		4
5		5
6		1
7		2
8	0.035	3
9		4
10		5
11		1
12		2
13	0.05	3
14		4
15		5
16		1
17		2
18	0.065	3
19		4
20		5

The VCFP isolator has been introduced to overcome this problem and control the amplification under near-field ground motions.

Here in order to investigate the effect of variation of D, seven near-field ground motions are used for sensitivity analysis of 120 VCFP isolator cases. The selected ground motions cover a wide variety of different intensities, frequency content and pulse periods in order to place performance of VCFP isolators under scrutiny. The detail information of the ground motions and their characteristics are presented in Table 4. As it seen, the pulse periods range from 1.4 to 5.7 seconds and peak ground acceleration varies between 0.46 g and 0.843 g.

The peak responses of the super structure without isolation system under the seven chosen ground motions have been presented in Table 5. These results can be used as a reference for evaluating effectiveness of different isolators.

5. Effect of sliding surface geometry on seismic performance of structure

5.1 Effect of mathematical function

Fig. 6 presents the hysteresis loops of case No. 12 of O4-2 and O6-2 isolators (D equals to 0.2 meters) under Imperial Valley 1979 ground motion as an example to show the effect of sliding surface geometry on seismic behavior of VCFP isolators. The hysteresis loop of FPS isolator with similar minimum friction coefficient and period ($f_{min} = 0.035$ and $T_0 = 2$ seconds) is also plotted to highlight the difference between FPS isolator and two different VCFP isolators.

Table 4 Summary of selected earthquakes data and characteristics

No	Record information			Record characteristics				Soil type
	Name	Year	Station	Magnitude	Pulse period (s)	PGA (g)	PGV (cm/s)	
1	Kobe	1995	Takarazuka	6.9	1.4	0.69	72	D
2	Erzincan	1992	Erzincan	6.7	2.7	0.515	95.5	D
3	Northridge	1994	Sylmar	6.7	3.1	0.843	122.7	C
4	Imperial Valley-06	1979	Elcentro array #7	6.5	4.2	0.46	108.8	D
5	Loma Prieta	1989	Saratoga	6.9	4.5	0.52	55.6	C
6	Landers	1992	Lucerne	7.3	5.1	0.79	140.3	C
7	Chi-Chi	1999	Tcu065	7.6	5.7	0.82	127.7	D

Table 5 Peak responses of un-isolated structure under seven near-field ground motions

Earthquake	No.	1	2	3	4	5	6	7
	Name	Kobe	Erzincan	Northridge	Imperial Valley-06	Loma Prieta	Landers	Chi-Chi
Structural response	Roof displacement (mm)	19.11	8.37	13.16	9.22	12.65	14.23	13.68
	Structural acceleration (g)	1.93	0.84	1.33	0.93	1.27	1.43	1.38

In this figure, hysteresis loop of O4 isolator possesses a hardening behavior as the slider moves away from its neutral position because the second derivate of sliding surface (the rate of variation of the stiffness) in O4 isolator is an increasing function with displacement. In comparison with FPS isolator with a linear function of isolator stiffness, the O4 isolator limits the excessive isolator displacements during high intensity and near field ground motion. The increasing stiffness causes slight residual displacements even in cases with high friction coefficient.

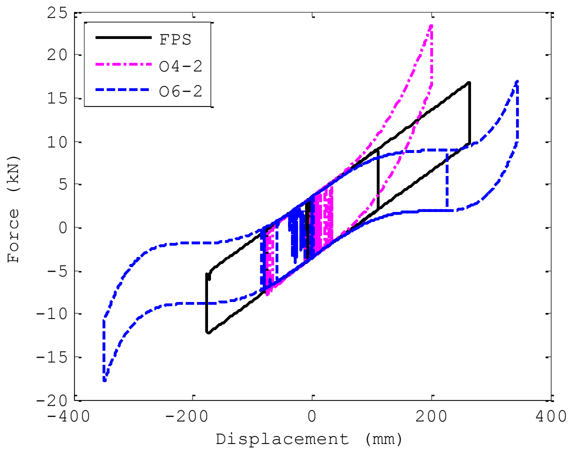

Fig. 6 Hysteresis loops of FPS, O4-2 and O6-2 isolators (case No. 12 of f_{min} = 0.05, T_0 = 2 sec) under Imperial Valley 1979 ground motion

In hysteresis loop of O6 isolator, stiffness between origin and $x = D$, is decreasing continuously to zero. In this phase due to zero restoring force isolator, transmitted acceleration to structure is limited. In low level of the input excitation slider does not exceed away from the inflection point and floor acceleration is controlled in compliance with immediate service objective for seismic performance design. By exceeding displacement more than $x = D$ in hysteresis loop of O6 isolator, its stiffness and restoring force is increased to control isolator displacements during high intensity near-fault ground motion.

5.2 Effect of specific displacement (D)

As described, specific displacement, *D*, is the distance from origin to the position that normalized isolator stiffness is equal to high amount of 4 (1/m) in O4 isolator, and represents changing point of the stiffness variation rate on sliding surface with normalized isolator stiffness equal to 0 (1/m) in O6 isolator.

Tables 7 and 8 show the effect of specific displacement (D) on seismic performance of isolated structure with VCFP subjected by seven near-fault ground motions. Results indicate that by using O4-3 average isolator displacement is increased 26.5 percent in comparison with O4-1, and average floor acceleration decreased about 35.4 percent. In compare to O4-2 these differences are reduced respectively to 2.9 and 21 percents. Fig. 7(a) shows the behavior of O4 isolator through hysteresis loops of case No. 8 with different specific displacements (O4-1, O4-2 and O4-3) under Imperial Valley 1979 ground motion.

The above results can be used for design purposes by selecting appropriate D in VCFP with O4 sliding function. By choosing a larger value for D, the isolator has a softer behavior in comparison with cases possessing smaller D. In this case, the isolator displacement is larger but transmitted force to superstructure will have lower magnitude. Accordingly to find out optimum value for D to simultaneous control of isolator displacement and floor acceleration, we need sensitivity analysis considering other design parameters as friction coefficient and initial period of isolation.

The related results to O6 sliding curvature in Table 7 show that, increasing specific displacement (D) has same effect on dynamic performance of structure with O4 sliding function. The average isolator displacements in O6-1 and O6-2, 10.4 and 3.2 percents are less than VCFP with O6-3 while the average floor accelerations respectively are 46 and 21 percents higher than isolated system with O6-3.

Fig. 7(b) shows the hysteresis loops of O6 isolator with different specific displacements (O6-1, O6-2 and O6-3) subjected by Imperial Valley 1979 ground motion. Similar to Fig. 7(a), increasing specific displacement, decreases isolator stiffness and results in larger maximum displacement.

It is noticeable that selection of specific displacement has more effective role on controlling peak floor acceleration in O6 sliding surface than O4, while it has more influence on maximum isolator displacement of O4 concave surface.

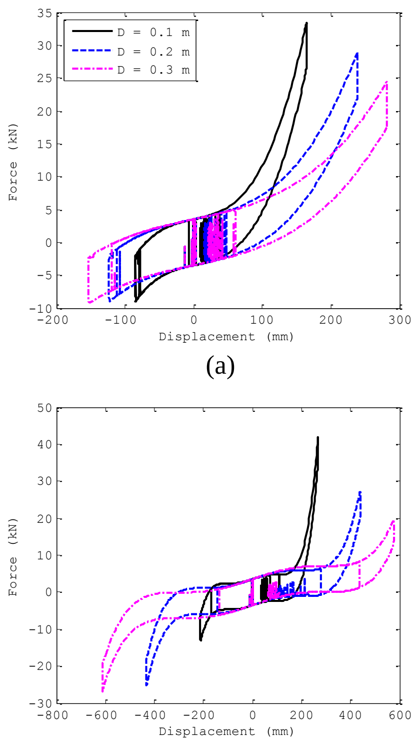

(a)

(b)

Fig. 7 Effect of specific displacement on hysteresis loops of case No. 8 of (a) O4 and (b) O6 isolators (f_{min} = 0.035, T_0 = 3 sec) under Imperial Valley 1979 ground motion

As it shown in Fig. 1, the value of D separates the acceleration and displacement control region and in compliance to Fig. 7(b), larger D in O6 sliding surface eliminates the floor acceleration impact due to entering to hardening phase. However, in VCFP with high friction coefficient, larger D causes high residual displacement that is undesirable.

It is of paramount importance to point out the optimum values of specific displacement for O6 depends on wide range of pulse periods and design parameters.

5.3 Effect of initial period

As an example to show the effect of initial period, Fig. 8 represents the hysteresis loops of O4 and O6 for different initial periods of isolation under Imperial Valley 1979 ground motion. As seen, any change in initial stiffness has a significant effect on seismic behavior of VCFP isolators.

Table 7 Average of structural responses of O4 isolators with different specific displacements, under seven near-fault ground motions (Disp. in mm, Accl. in g)

VCFP type	O4 Isolator					
Specific Displacement, D (m)	0.1		0.2		0.3	
Structural Response	Displ.	Accl.	Displ.	Accl.	Displ.	Accl.
Kobe	189.95	1.15	213.56	0.66	199.04	0.46
Erzincan	189.44	1.12	255.63	0.91	303.78	0.81
Northridge	214.80	1.44	294.39	1.26	329.02	0.97
Imperial Valley-06	137.84	0.57	187.21	0.51	218.19	0.48
Loma Prieta	98.76	0.43	99.48	0.28	99.15	0.26
Landers	34.71	0.28	35.79	0.28	36.02	0.28
Chichi	397.40	5.17	520.17	4.81	414.67	1.45

Table 8 Average of structural responses of O6 isolators with different specific displacements, under seven near-fault ground motions (Disp. in mm, Accl. in g)

VCFP type	O6 Isolator					
Specific Displacement, D (m)	0.1		0.2		0.3	
Structural Response	Displ.	Accl.	Displ.	Accl.	Displ.	Accl.
Kobe	180.81	0.68	197.61	0.34	194.08	0.33
Erzincan	281.78	1.56	378.94	0.65	384.21	0.34
Northridge	289.81	2.14	346.69	0.56	351.67	0.39
Imperial Valley-06	230.45	0.73	334.37	0.56	400.89	0.52
Loma Prieta	110.71	0.25	104.95	0.24	103.84	0.24
Landers	211.55	0.28	36.32	0.28	36.26	0.28
Chichi	282.05	4.51	334.80	2.00	343.40	0.84

By paying attention to Eq. (13), selecting initial period equal to 1 second for O4 isolator leads to an initial normalized isolator stiffness almost equal to 4 (1/m). In this case, the coefficeint p_1 would be equal to zero (see Eq. (8)) and the sliding surface mathematical function is changed to order 2 polynomial function (circle) which is a FPS bearing. This behaviour could be observed in hysteresis loop of O4-3 isolator case with T_0 = 1 sec in Fig. 8(a). Hysteresis behavior of the other cases ($T_0 \neq 1$) has not consistent pattern with variation of initial period.

For O6 isolator, Fig. 8(b) shows that O6 isolator with initial period of 1 second leads to an isolator with high initial stiffness that strictly prevents sliding and cause high transmitted force and structural acceleration. The isolators with long initial period generally causes less structural acceleration and higher isolator displacements. Further, Tables 9-10 represent average of structural responses of VCFP isolators with of different initial periods, under seven near-fault ground motions. Relative standard deviation of data shows that structural responses strongly depend on other design parameters and input excitation characteristics. Accordingly, it is not an easy task to determine a unique value as optimum initial stiffness.

Herein, the most appropriate combination to control maximum isolator displacement and roof acceleration simultaneously is related to O4 bearing with long initial periods varies between 4 and 5 seconds when it has high friction sliding.

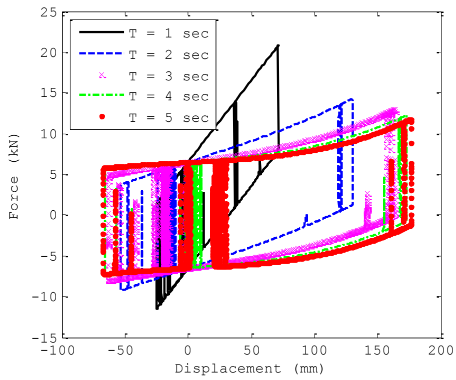

(a)

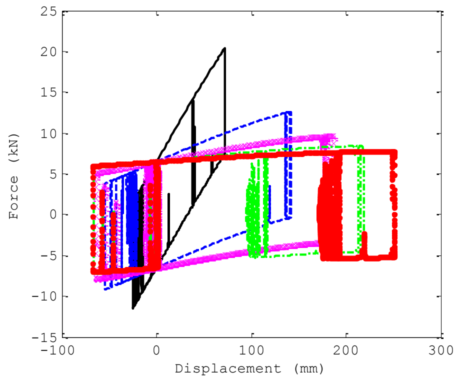

(b)

Fig. 8 Effect of initial period of isolation on hysteresis loops of (a) O4-3 and (b) O6-3 isolators with f_{min} = 0.065 under Imperial Valley 1979 ground motion

Table 9 Average of structural responses of O4 isolators cases with different initial periods, under seven near-fault ground motions (Disp. in mm, Accl. in g)

VCFP Type		O4				
Initial Period		1	2	3	4	5
Kobe	Displ.	172.77	238.09	212.33	194.74	186.33
	Accl.	0.82	0.88	0.76	0.68	0.64
Northridge	Displ.	150.53	253.20	275.66	282.80	285.89
	Accl.	0.72	0.91	1.00	1.04	1.06
Loma Prieta	Displ.	171.81	299.82	307.30	308.70	309.37
	Accl.	0.81	1.27	1.33	1.35	1.36
Chichi	Displ.	91.59	175.89	205.28	214.44	218.20
	Accl.	0.46	0.48	0.54	0.56	0.57
Erzincan	Displ.	60.33	104.40	108.07	110.65	112.20
	Accl.	0.35	0.33	0.31	0.31	0.30
Imperial Valley-06	Displ.	26.20	33.14	37.57	39.69	40.94
	Accl.	0.30	0.28	0.27	0.27	0.26
Landers	Displ.	596.41	468.56	413.56	379.67	362.20
	Accl.	2.47	4.72	4.25	3.88	3.74

Table 10 Average of structural responses of O6 isolators cases with different initial periods, under seven near-fault ground motions (Disp. in mm, Accl. in g)

VCFP Type		O6				
Initial Period		1	2	3	4	5
Kobe	Displ.	223.75	222.23	176.12	166.58	165.48
	Accl.	1.13	0.43	0.23	0.23	0.23
Northridge	Displ.	183.53	356.68	377.27	404.11	419.96
	Accl.	0.84	1.07	0.91	0.76	0.68
Loma Prieta	Displ.	226.03	372.43	358.13	340.37	350.00
	Accl.	1.23	1.38	1.05	0.81	0.68
Chichi	Displ.	102.09	276.22	364.28	417.13	449.77
	Accl.	0.40	0.57	0.66	0.70	0.69
Erzincan	Displ.	72.95	102.17	111.69	119.84	125.86
	Accl.	0.36	0.22	0.22	0.21	0.21
Imperial Valley-06	Displ.	26.24	33.75	38.61	41.00	42.32
	Accl.	0.30	0.28	0.27	0.27	0.26
Landers	Displ.	404.44	348.33	277.16	267.35	303.13
	Accl.	6.62	3.58	1.36	0.36	0.35

5.4 Effect of friction coefficient

Friction coefficient indicates the roughness of sliding surface that provide a resistance force against sliding of two surfaces. It is important design parameter which plays a predominant role in seismic performance of sliding isolators. The effect of friction coefficient on seismic behavior of VCFP isolators has been presented in Fig. 9. It shows hysteresis loops of O4-2 and O6-2 cases with T_0 equal to 2 seconds and different friction coefficient under Imperial

Valley 1979 ground motion.

As shown, selecting higher value for minmum friction coefficient limits movement of the slider away from the origin. O4 isolator can easily deal with the problem of residual displacement due to its increasing restoring force starting at the very beginning of sliding. This hardening phase increases the restoring force even for high friction coefficents.

For O6 isolator which its sliding surface begins with the softening phase continouing till a point with zero stiffness, different effect for friction coefficient is observed. According to listed responses of VCFP isolators in Table 11, best responses of O6 isolator under seven near-fault ground motions are achieved from two friction coefficients equal to 0.035 and 0.05.

5.5 Comparison the results

In order to evaluate the simultaneous effect of described parameters on seismic performance of isolated structure with VCFP, the maximum response of system with 120 different bearings are compared with the corresponding cases of FPS isolators. Fig. 10 illustrates the peak floor acceleration and maximum isolator displacement of structure mounted on 20 cases of each VCFP and FPS isolator, listed in Table 3 under Imperial Valley 1979 ground motion. Each graph represents the related VCFP with O4 and O6 sliding functions with three different geometrical properties in Table 2.

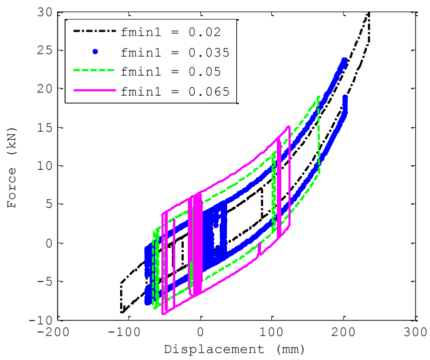

(a)

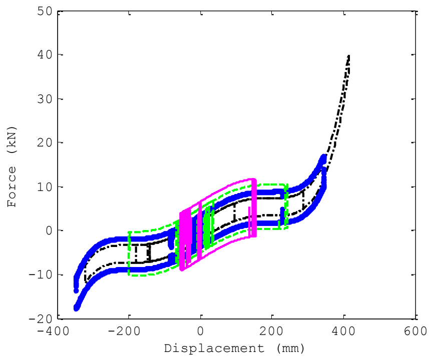

(b)

Fig. 9 An example of effect of friction coefficient on hysteresis loops of (a) O4-2 and (b) O6-2 isolators with T_0 = 2 under Imperial Valley 1979 ground motion

The results indicate that the maximum isolator displacement of structure with O4 isolator is reduced in comparison with FPS isolator. In more than 80 percent of O4-1 cases, the maximum displacement is less than FPS bearings. However, the peak floor acceleration in 72 percent of cases is higher than response of structures isolated with FPS systems.

Maximum displacement of O6 isolator in 62 percent of cases is higher than corresponding FPS isolator while its peak floor acceleration in 56 percent cases is lower than FPS system. As it described before, specific displacement (D) and friction coefficient have a significant role in seismic behavior of O6 and O4 isolators.

Above results can be used for optimum design of VCFP isolators with O4 or O6 functions. In VCFP isolators with O4 function, the specific displacement of 0.3 meters with long initial period like 4 to 5 seconds in combination with minimum friction coefficient more than 0.05 can reduce both peak floor acceleration and maximum isolator displacement. For O6 isolator combination of specific displacement between 0.2 to 0.3 meters, initial period more than 2 seconds and minimum friction coefficient between 0.03 to 0.05 exhibit the best structural responses.

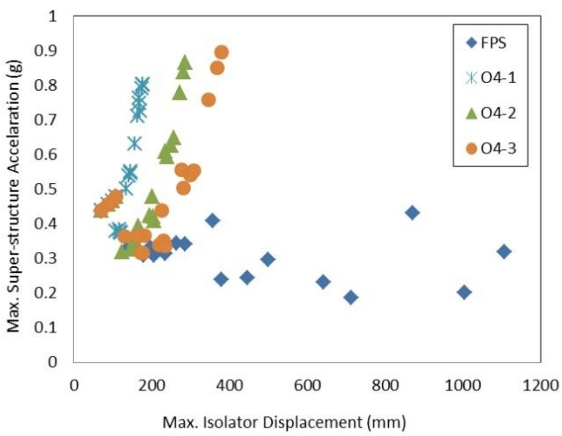

(a) O4

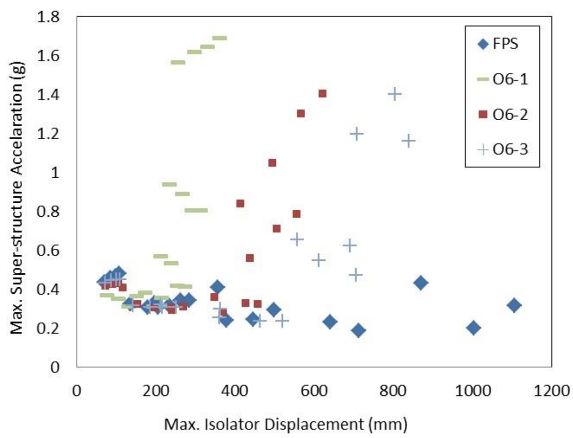

(b) O6

Fig. 10 The maximum responses of 20 cases of three different (a) O4 and (b) O6 isolators under Imperial Valley 1979 ground motion

Table 11 Average of structural responses of VCFP isolators cases with different friction Coefficients, under seven near-fault ground motions (Disp. in mm, Accl. in g)

VCFP Type		O4				O6			
Friction Corficient		0.02	0.035	0.05	0.065	0.02	0.035	0.05	0.065
Kobe	Displ.	258.77	218.84	180.38	145.42	225.49	203.56	178.65	155.64
	Accl.	1.14	0.82	0.59	0.47	0.59	0.47	0.36	0.37
Northridge	Displ.	299.41	270	233.54	195.51	422.9	383.61	320.34	266.39
	Accl.	1.30	1.0531	0.8094	0.6328	1.3194	0.9698	0.6418	0.4722
Loma Prieta	Displ.	328.23	297.55	263.72	228.13	411.36	352.99	301.87	251.34
	Accl.	1.56	1.3177	1.1036	0.9055	1.5674	1.1831	0.8275	0.5539
Chichi	Displ.	231.45	201.23	164.58	127.07	442.35	377.9	287.97	179.39
	Accl.	0.71	0.5757	0.4365	0.3675	1.1167	0.5998	0.3621	0.3381
Erzincan	Displ.	158.91	110.55	72.355	54.703	170.28	119.08	79.413	57.229
	Accl.	0.46	0.2577	0.2629	0.3029	0.2021	0.209	0.2608	0.3029
Imperial Valley-06	Displ.	57.15	35.317	27.738	21.827	59.765	35.801	28.08	21.887
	Accl.	0.20	0.2443	0.3042	0.3619	0.1937	0.2439	0.3039	0.3616
Landers	Displ.	532.77	480.78	408.65	354.12	321.93	316.29	329.05	313.06
	Accl.	5.15	4.5171	3.1234	2.457	3.4901	2.4109	2.1367	1.7736

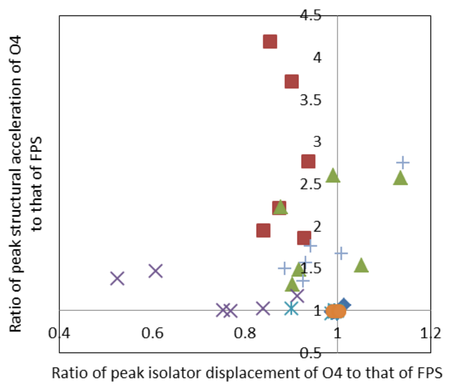

(a) O4

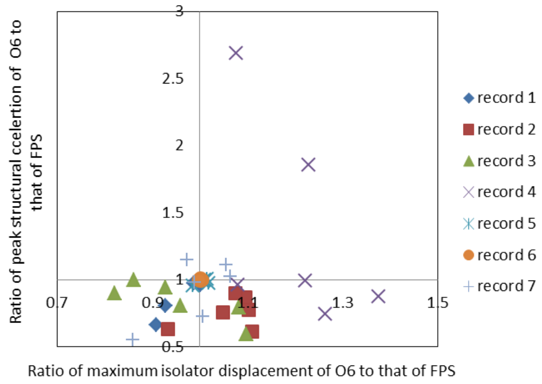

(b) O6

Fig. 11 Average ratio of structural responses of VCFP optimum isolator to that of corresponding FPS isolator under seven near-fault ground motions

Beside desire performance of isolation, another important factor specially to select sliding surface function is the intensity of maximum probable earthquakes. Fig. 11 represents average ratio of structural responses of O4 and O6 optimum isolators to that of corresponding FPS isolator under seven chosen near-fault ground motions. As it shown, for O4 isolator best results are observed under Imperial Valley ground motion which has the least PGA and worst responses are observed under Chi-Chi and Northridge ground motions which are records with almost highest PGA level.

Contrarily to control maximum floor acceleration simultaneously as isolator displacement, the seismic performance of structures with O6 isolators under stronger ground motions such as Chi-Chi and Northridge ground motions is better than the behavior of isolators under weaker intensity ground motion.

6. Conclusions

Variable Curvature Friction Pendulum (VCFP) bearing is possessing non-spherical sliding surface with variable curvature. One challenging issue in the subject of application of VCFP isolators is its design process, that takes more time and energy than conventional isolators due to numbers of design parameters. Therefore, research works, especially in sensitivity analysis field and experimental investigation needs to be carried out in order to understand the behavior of the VCFP isolators and finding the optimum values of design parameters.

Here, a parametric study has been conducted on 120 cases of different VCFP isolators and compared to corresponding FPS cases with two types of sliding surface. In order to control excessive induced responses of isolated structures subjected to near-fault ground motions, two different polynomial functions of order 4 (O4) and order 6 (O6) were selected in different cases. The desired performance is defined as controlling floor acceleration as well as isolator displacement under the action of near-fault ground motions.

Some of the important achievements in this study are concluded as follows:

- The most appropriate function to achieve desired performance of isolated structure is O4 when subjected to low intensity level ground motion and it is O6 when subjected to great strong motions.
- Appropriate specific displacement (D) for O4 isolator is 0.3 meter and for O6 isolator is between 0.2 and 0.3 meters.
- The seismic responses of isolated structure are closer to desired performance for O4 when initial period of bearing (T_0) is more than 4 seconds and for O6 isolator when it is more than 2 seconds.
- Minimum friction coefficient more than 0.05 for O4 isolator and between 0.035 and 0.05 for O6 isolator are the optimum range for these two functions.
- The best seismic performance of VCFP isolators studied in this paper under near-fault ground motions belongs to O6 isolators that effectively reduce inter-story drift by reduction of structural acceleration.

References

Calvi, P.M. and Ruggiero, D.M. (2016), “Numerical modelling of variable friction sliding base isolators”, *Bull. Earthq. Eng.*, **14** (2), 549-568.

Fakhouri, M.Y. and Igarashi, A. (2013), “Multiple‐slider surfaces bearing for seismic retrofitting of frame structures with soft first stories”, *Earthq. Eng. Struct. D.*, **42**(1),145-161.

Fallahian, M., Khoshnoudian, F. and Loghman, V. (2015), “Torsionally seismic behavior of triple concave friction pendulum bearing”, *Adv. Struct. Eng.*, **18**(12), 2151-2166.

FEMA, NEHRP. (2003), Recommended Provisions for Seismic Regulations for New Buildings and Other Structures (FEMA 450) , Washington, DC, USA.

Fenz, D.M. and Constantinou., M.C. (2008a), *Mechanical Behavior of Multi-Spherical Sliding Bearings*, Multidisciplinary Center for Earthquake Engineering Research.

Fenz, D.M. (2008), *Development, Implementation and Verification of Dynamic Analysis Models for Multi-spherical Sliding Bearings*, ProQuest.

Fenz, D.M. and Constantinou, M.C. (2008b), “Modeling triple friction pendulum bearings for response-history analysis”, *Earthq. Spectra*, **24**(4), 1011-1028.

Gillich, G.R., Minda, A.A., GIillich, N., Jurcau, S.C. and Iavornic, C.M. (2012), “Robust friction pendulum with parameterized sliding surfaces”, *Proceedings of the 1st International Conference on Sustainable Development, Sustainable Chemical Industry, Pollution, Hazards and Environment.*

Kong, D., Fan, F. and Zhi, X. (2014), “Seismic performance of single-layer lattice shells with VF-FPB”, *Int. J. Steel Struct.*, **14** (4), 901-911.

Lu, L.Y. and Hsu, C.C. (2013), “Experimental study of variable-frequency rocking bearings for near-fault seismic isolation”, *Eng. Struct.*, **46**, 116-129.

Lu, L.Y., Lee, T.Y., Juang, S.Y. and Yeh, S.W. (2013), “Polynomial friction pendulum isolators (PFPIs) for building floor isolation: An experimental and theoretical study”, *Eng. Struct.*, **56**, 970-982.

Lu, L.Y., Lee, T.Y. and Yeh, S.W. (2011), “Theory and experimental study for sliding isolators with variable curvature”, *Earthq. Eng. Struct. D.*, **40**(14), 1609-1627.

Moeindarbari, H. and Taghikhany, T. (2014), “Seismic optimum design of triple friction pendulum bearing subjected to near-fault pulse-like ground motions”, *Struct. Multidiscip. O.*, **50**(4), 701-716.

Mostaghel, N. and Tanbakuchi. J. (1983), “Response of sliding structures to earthquake support motion”, *Earthq. Eng. Struct. D.*, **11**(6), 729-748.

Panchal, V.R. and Jangid, R.S. (2008a), “Variable friction pendulum system for near‐fault ground motions”, *Struct. Control Health Monit.*, **15**(4), 568-584.

Panchal, V.R. and Jangid, R.S. (2008b), “Variable friction pendulum system for seismic isolation of liquid storage tanks”, *Nucl. Eng. Des.*, **238** (6), 1304-1315.

Pranesh, M. and Sinha, R. (2000), “VFPI: an isolation device for aseismic design”, *Earthq. Eng. Struct. D.*, **29**(5), 603-627.

Shahbazi, P., Moeindarbari, H. and Taghikhany, T. (2013), “Comparative study on the behavior of double variable curvature friction pendulum systems”, *Proceeding of the 13th World Conference on Seismic Isolation, Energy Dissipation and Active Vibration Control of Structures*, Sendai, Japan, September 24-27.

Shahbazi, P. and Taghikhany, T. (2014), “Comparative study on the behavior of variable curvature friction pendulum isolator”, *Proceeding of the 2nd European Conference on Earthquake Engineering and Seismology (2ECEES)*, Istanbul, Turkey, August 24-29.

Sinha, R. and Pranesh, M. (1998), “FPS isolator for structural vibration control”, *Proceeding of the Int. Conf. on Theoretical, Applied, Computational and Experimental Mechanics (CD Volume)*.

Tsai, C.S., Chiang, T.C. and Chen, B.J. (2003), “Finite element formulations and theoretical study for variable curvature friction pendulum system”, *Eng. Struct.*, **25**(14),1719-1730.

Tsai, C.S., Chiang, T.C. and Chen, B.J. (2004), “Experimental study for multiple friction pendulum system”, *Proceedings of the 13th World Conference on Earthquake Engineering*.

CY